TECHNICAL REPORT
10 April 1981

Pueblo Viejo-Quixal Seismograph Network
13 February 1979 through 10 March 1981

Submitted to:

Ing. Edgar Celada
Instituto Nacional de Electrificacion
6a. Ave. 2-73, Zona 4
Guatemala City, GUATEMALA

Prepared by:

Dr. Tosimatu Matumoto
Dr. Jung Joon Kim
Mr. Lewis Rabb
Marine Science Institute
Geophysics Laboratory
700 The Strand
Galveston, Texas 77550

The University of Texas Institute for Geophysics Contribution No. 560.

CONTENTS

1. INTRODUCTION

During the 24 month period from 13 February 1979 through 10 March 1981, approximately 4400 local and regional earthquakes were recorded by the Pueblo Viejo-Quixal seismograph network. Of the 4400 events recorded, 2600 foci were located. This report is to summarize the results of the seismic monitoring program during the period mentioned above. During this period, six regional trends of activities were delinieated, two of which were located in the vicinity of the Pueblo Viejo Dam Site. Accumulation of the recorded earthquakes now permit us to draw a conclusion on the recurrence time with an acceptable confidence limit.

To complement the data from the Pueblo Viejo-Quixal network, the information from the World-Wide Standardized seismograph network (WWSSN) complied by the National Earthquake Information Service (NEIS), U.S. Geological Survey is incorporated in our analysis as needed.

Three preliminary reports (#1, 25 April 1979, #2, 10 November 1979; and #3, 29 August 1980) have been submitted to INDE during the past 2 year contract period. A part of the discussions included in these reports will be duplicated in this text as needed.

2. TECTONIC SETTING

Guatemala is located in the central portion of northern Central America. Northern Central America is defined as the land and continental shelf area which extends from Isthmus of Tehuantepec in southern Mexico to central Nicaragua. It is distinguished from the land area of southern Central America (southern Nicaragua, Costa Rica, and Panama) primarily on the basis of crustal structure and inferred age of formation. Northern Central America is believed to be underlain by a continental type crust with the basement as old as Paleozoic. In contrast, Dengo (1967) suggested that southern Central America formed in late Jurassic to early Cretaceous time as a raised block of thickened oceanic crust.

Central America is a part of the circum-Pacific "Ring of Fire", a zone of intense seismic and volcanic activity. The intense seismic and volcanic activity of Central America can be explained as a consequence of the collision of three major plates; Cocos, North American, and Caribbean plates. According to focal mechanism studies (Molnar and Sykes, 1969; Dean and Drake, 1978), the Cocos plate is moving in a northeasterly direction and is being subducted beneath the Caribbean plate which is moving eastward with respect to the North American plate. The movement of these plates is believed to result in several prominent tectonic features such as the Middle America trench, a chain of active Quatenary volcanoes, and numerous near surface faults that strike parallel, subparallel, and perpendicular to the Middle America trench such as the Nicaragua graben. The seismicity associated with this subduction of the Cocos plate is probably contributing the largest portion of the

seismic energy in and near Guatemala. Although the most of the major earthquakes along the subduction zone are located off the Pacific coast of Guatemala and relatively harmless, some of the earthquakes that occurred in the immediate proximity of large cities, depsite the magnitude was relatively smaller, proved to be extremely destructive. The 23 December 1972 Managua earthquake (Ms=6.2) was one of the examples in recent years.

A series of east-west trending fault systems that transect Guatemala is very important in terms of tectonics as well as the seismic risk analysis for the Pueblo Viejo-Quixal project. This includes the Cuilo-Chixoy-Polochic fault, the Motagua fault, and the Jocotan-Chamelecon fault. The plate boundary east of Guatemala seems reasonably well defined from the pattern of seismic activity associated with the Cayman trough; however, the precise location of the westward extension through Guatemala had been a matter of some controversy. Muehlberger and Ritchie (1975) proposed that the CCP fault is the active boundary and that it bends southward near the Guatemala-Mexico border. The 4 February 1976 Guatemala earthquake (M=7.5) ruptured the crust 240 km along the Motagua fault and indicated that the Motagua fault is at least one of the currently active boundaries between the North American and the Caribbean plates. The data from the Pueblo Viejo-Quixal seismograph network, nested around the CCP fault, however, delineated significant activity along this fault system. Therefore, it is now believed that the plate boundary is defined by not a single fault but by a series of subparallel systems including the Motagua fault, the CCP fault and possibly Jocotan-Chamelecon fault.

The wedge-shaped, western most section of the Caribbean plate is pinched between the North American and the Cocos plates. As the Caribbean plate moves eastward, the unstable wedge tends to splinter with N-S or NE-SW trends. The Mexico fault and the Honduran graben are some of the examples of such a splintering. The Guatemala earthquake also activated N-S trending fault (Matumoto and Latham, 1976) near Tecpan, approximately 40 km west of Guatemala City. Some of the N-S trending activities seem to have been developed beyond the Motagua fault. Usually these faults show a normal faulting to take up a E-W tensional feature caused by the eastward motion of the Caribbean plate. The fault plane solutions of the N-S trending activity uncovered in the vicinity of the dam site are in accordance with this regional stress pattern.

3. THE PUEBLO VIEJO-QUIXAL SEISMOGRAPH NETWORK

3.1. DESCRIPTION OF THE SEISMOGRAPH NETWORK

Seven station Pueblo Viejo-Quixal Seismograph Network was installed in February 1979 to monitor the seismic activity in the area associated with the Pueblo Viejo-Quixal hydroelectric project (Figure 1 and Table 1). To insure the accurate timing resolution, the signals from the remote stations are transmitted back to the central recording station and registered on the drum recorder (Figure 2). To provide higher timing resolution required for the engineering application, a tape recorder system and memory-trigger system were augmented to the network in May 1979. After the installation, the signal from a station has been recorded both on drum recorder and tape recorder. This dual recording system not only improved the timing resolution, but also provided a reliable, fail-safe back-up for the continuous recording.

As shown in Figure 1, the stations 1 through 3 are located closely together near the dam site. These closely spaced inner cluster stations are providing the highest perceptibility for microearthquakes and greatest precision of epicenter determination in the vicinity of the dam site. Stations 4 through 7, on the other hand, are distributed at greater distances to cover the area up to 40 km from the dam site. These peripheral stations assure a coverage of wider area and provide necessary information for the study of the fault plane solutions.

Operated at 78 db gain (the operating level for the Pueblo Viejo-Quixal network), an earthquake with magnitude 0.5 or greater in Richter scale will be recorded within the inner cluster stations. The standard error of an epicenter determination within the inner cluster is expected

to be less than 500 meters. Within 40 km range, the network will be able to register an earthquake with magnitude 2.5 and greater.

Comparison of the number of earthquake recorded by the Pueblo Viejo-Quixal network and those recorded by the World-Wide Network (WWSSN) support the perceptible magnitude described above. During 24 month period of November 1978 through October 1980, 35 events were located by WWSSN within the area covered by the Pueblo Viejo-Quixal network. This area is approximately identical shown in Figure 4. The magnitude of the perceptible earthquake by WWSSN in this region is estimated at 4.5. The frequency-magnitude relation indicates that the number of the perceptible earthquakes increases approximately 7 to 9 times if the perceptible magnitude is lowered by one scale. Therefore the events count of 35 at magnitude 4.5 can be accounted for roughly 1700 to 2800 earthquakes for the perceptible magnitude 2.5. This estimated count agrees well with the number of 2600 located earthquakes by the Pueblo Viejo-Quixal network.

3.2. OPERATION OF THE SEISMOGRAPH NETWORK

3.2.1 General Comments

Since the installation of the Pueblo Viejo-Quixal seismograph network in February 1979, we have experienced several setbacks. Of the most severe nature was that station 7 and 6 were destroyed by the local bandits on 27 March 1979 and 7 March 1981 respectively. Station 7 was relocated twice on 29 April 1979 and 5 October 1979. Due to high noise level, station 3 was relocated on 28 April 1979 We expect to relocate and reestablish station 6 in late April 1981.

During the 2 years of operation, the most frequently experienced problem way maintenance of the remote stations. Extremely humid climate, inaccessable topography and to some extent background of the maintenance crew may have attributed to the problem. Many times it was also not possible to send a technician from Texas to take care of the problem immediately. At the central recording station, the performance of the equipment purchased from Kinemetrics and Teledyne Geotech (the drum recorder and time code module) respectively were worse than we anticipated.

3.2.2 Operation During The Period From April 1980 Through March 1981

The Figure 3A, 3B, and 3C contained in this report reflect the individual station performance for each month. Dark shaded areas which represent station "down" time were shaded when we were unable to determine the epicentral locations of the events due to insufficient data. The actual problem may have been in the central recording station, but in order to maintain graph continuity and simplicity from previous reports, details could not be represented graphically. Comments concerning the drum recording system have been made for each month to augment the graphs and present a more complete assessment. Please note that the shaded areas and the operation of the drum recorders are not directly correlated.

Reviewing the performance over the last year, I have noticed some things of general concern. The "down time" of the network was highest in May, June and July of 1980. Most of this was due to the inoperable condition of the remote sites. As the year progressed, the "down time" decreased immensely indicating an extensive maintenance period. Stations 1Z, 1N, 1E, 6 and 7 however, were continually dropping in and out of operation throughout the year. Recently however, it was found that there was only one solar panel charging the batter at station 7 which will cause intermittent drops in voltage thereby causing transmission failure.

The overall operation of the network for this time period was better than expected. Over 2000 earthquakes were located using both the drum records and the tape recording system. The drum records generally exhibited events with good clarity and high sensitivity. The tape recording system enables us to study in greater detail the waveforms of each individual event. The last five months indicated almost perfect performance with little or no maintenance required.

There are certain precautions that can be taken to minimize station down time. Checking the receiver output of the central recording station will determine whether the remote site is functioning or not. If a signal is not received, or it is not frequency modulated, a trip to the remote site must be made. If closer attention is devoted to the operational condition of each drum, the quality of data can be improved immensely. Things such as ink supply tubes, pens and pen mechanisms and the threaded drive screw should be checked and cleaned on a bi-weekly or monthly basis (whenever it appears necessary).

Station 5 seems to always produce a good drum record. Using the condition of this drum as a model, each station record should look like that. Note the pen trace thickness, ink supply, uniformness of trace spacing throughout the page and the clarity of the time mark.

4. DISTRIBUTIONS OF THE EARTHQUAKES RECORDED BY THE PUEBLO VIEJO-QUIXAL SEISMOGRAPH NETWORK

4.1. DATA ANALYSIS

A procedure for data analysis was described in the previous reports (Preliminary report #1, p.2-4; #2, p.14-17; #3, p.5-8). It was emphasized in these reports that the accuracy of the epicenter determination is affected by the various factors such as the number of the stations recorded, distribution of recording stations, signal-to-noise ratio, the station correction, the crustal model and timing resolution.

To draw a meaningful conclusion from an ensemble of data, therefore, all the data should not be handled equally, but only the data with higher accuracy should be selected.

As the criteria to select the reliable earthquakes, two indices were used to study the distribution of earthquakes. IQ factor: This factor is ranging from 1 through 5 for the local earthquakes and decreasing number indicates more reliable epicenter determination. This factor is assigned based on the number of the stations recorded and sharpness of the first onset (S/N ratio). The exceptions for this rule are a distant earthquake (IQ=6) and an explosion event (IQ=7). Table 2 gives the number of events classified by IQ. Standard error: When the number of the readings is more than the number of unknowns, the epicenter program based on the least square fitting gives the standard error for the calculated results. An error for the origin time is usually selected as an index for selection.

4.2. THE REGIONAL SEISMICITY

Distribution of earthquakes that occurred during the period from 13 February 1979 through 10 March 1981 is illustrated in Figure 4. Only the events that meet the following conditions are selected:

1. IQ was equal to or less than 3
2. S (the standard deviation in the calculation) was less than 0.5
3. The depth was between 0 to 20 km.

As a consequence, only 94 events are plotted in this figure. The heavy lines in Figure 4 show the regional fault systems and the lighter solid lines illustrate the contact between two different geological elements (after Bonis et al., 1970).

The general trend is almost identical to the plot shown in the Preliminary Report No. 3 (the data included was up to 5 April 1980 and only few events recorded during April 1980 and March 1981). This is partially due to the fact that the maintenance of the network suffered a number of problems recently (see 3.2.2.), and probably some of the events weren't recorded properly, or even if recorded the epicenter determinations did not satisfy the selection criteria described above. Accordingly we can draw the same conclusion as reported in the last report:

a) Well-defined activity distributed along the Chixoy-Polochic fault. The distribution extends from 30 km east to 35 km west of station trending nearly east-west.

b) Along this lineation, two dense clusters are observed. One of the heaviest concentration of the earthquakes is located near the Pueblo Viejo-Quixal project area. Within this cluster, we can possibly define two trends: One with north-south orientation, and one trending northwest-southwest can be recognized. The more detailed nature of these distributions will be discussed in the section 4.3.

c) Another marked cluster along the Chixoy-Polochic fault is located approximately 10 to 15 km west of station 1. Weakly defined north-south orientation can be observed.

d) A line of earthquakes with east-west orientation emerged north of station 5. As shown in Figure 4, no immediate correlation to the geological feature is observed.

e) To the south, a weakly defined trend along the Motagua fault is observed. To compare the seismicity levels of the Chixoy-Polochic fault and the Motagua fault, one has to consider that the perceptibility within the inner stations is significantly higher than those at the periphery of the network. Within the inner stations, the network will detect an event with the magnitude 0.5 and greater as compared to possibly 1.5 to 2.0 along the Motagua fault. This means that approximately 10 to 20 times more events will be detected at the center of the network as compared to the area along the Motagua fault. Even counting this difference on the detection levels, the activity is significantly lower along the Motagua fault. Especially

the absence of the events east of the meridian $90^{o}30'$ is remarkable. This means that the Motagua fault went through the readjustment period (aftershock period) following the Guatemala earthquake, and possibly started to accumulate the energy for another earthquake.

4.3. THE SEISMICITY IN THE VICINITY OF THE PUEBLO VIEJO DAM SITE

Figure 5A and 5B exhibit the earthquakes located near the Pueblo Viejo dam site. All the explosion events are eliminated from this figure to simplify the illustration. Scattered distribution of the earthquakes makes it difficult to define linear trend of earthquakes with confidence. However, two possible trends can be observed. One is running with north-south orientation from east of station 1 through south of station 2, and the other is striking northeast-southwest. The latter is probably divided into two subparallel trends; one running from 4 km south of Santo Cruz to south of the dam site and the other located north-west of the dam site and station 2. Delineation of these two seismic trends is supported by the study of composite fault plane solution (described in the next section). Two solutions obtained in the fault plane solutions are N 17^{o}W and N 48^{o}E respectively (Figure 6), and are roughly parallel to the directions of active seismic zones mentioned above. Both linear trends may have lengths up to 10 km long.

4.4 COMPOSITE FAULT PLANE SOLUTIONS

The current station coverage in Guatemala is insufficient for the construction of focal mechanism (or fault plane) solutions for individual events; however, it is possible to combine the arrivals from many events within a given tectonic regime and construct a single composite fault plane solution.

Figure 6 shows an upper-hemisphere equal-area projection of all

the reliable first motions for events shown in Figure 6. A closed circle shows compression and an open circle illustrates dilation. This composite fault plane solutions demonstrate that the earthquakes are a combination of normal faulting and strike-slip mechanism. Two solutions illustrated in Figure 6 are:

Fault plane #1	Strike N 17^{o}W	Dip 30^{o}E
Fault plane #2	Strike N 48^{o}E	Dip 35^{o}NW

Along the fault plane #1, we do expect the motion of right-lateral strike-slip and east downthrown normal faulting. For the fault plane #2, the anticipated movements are left-lateral strike-slip and northwest downthrown normal faulting. These solutions also suggest the regional stress pattern of east-west tension and north-south compression. These solutions are in general agreement with the study by Burkhart (1978) based on Landsat imaginary that support the regional movement expected from the eastward motion of the Caribbean and north to North-eastward motion of the Cocos plates.

It is emphasized that a linear trend revealed by microearthquakes frequently does not correspond to any visible faulting observed at the surface. A seismically active zone is not necessarily old enough so that a visible displacement has already been developed to the surface. Especially, if a linear trend defined by microearthquakes is short in distance, it is likely that this rupture zone has never experienced a major earthquake that provides a major offset that becomes measurable at the surface. Therefore, existence of possible rupture zones, as postulated in this report, should not be ignored on the basis that no visible fault has been found.

Utsu (1968) delivered the relation between surface magnitude MS and the length of aftershock zone l as follows:

$$Ms = 2 \log l \text{ (km)} + 3.6 \qquad (1)$$

It is generally accepted that the aftershock zone represents the area in which the rupture occured. Therefore, we can consider l as the length of the rupture zone as well. If we take the value of l at 10 km, the magnitude (Ms) calculated from equation (1) is estimated at 5.6. Since the value $l = 10$ km represents the maximum length of possible rupture zones (both for north-south and northeast-southwest trending zones), $Ms = 5.6$ gives the maximum magnitude we would expect from these local faults.

5. MAGNITUDE VERSUS FREQUENCY RELATION AND ESTIMATION OF RECURRENCE TIME

5.1. GENERAL COMMENTS

An empirical relation between the number of earthquakes and magnitude provides a useful clue to estimate the level of the seismic activity in the given area and the recurrence time of an earthquake as the function of magnitude. Usually the relation, known as the Gutenberg-Richter's formula (1954), is given as follows:

$$\log N = a - bM$$

Where N is the number of earthquakes with magnitude equal to or greater than the magnitude M, and a and b are constants. If N is normalized for the annual count, 1/N gives the recurrence time.

This relation, however, has several limitations before one can use and draw a conclusion. Abuse of this relation tends to lead a conclusion of no reliable foundation.

(1) This empirical formula is applicable to the ensemble of the earthquakes of random distribution. Any series of events which does not follow this criterion, such as the aftershock sequence following a major earthquake should not be applied for this formula.

(2) This relation is statistically defined empirical formula. The confidence limit of the coefficient b, for instance, varies significantly by the sample size. Aki (1965) calculated the confidence limit of the coefficient b as a function of the confidence level and the sample size. For 95% of confidence level, the confidence limit of b is $b(1\pm0.28)$ for the sample size of 50 events, and $b(1\pm0.03)$ for the sample size of 4000. This means that if we try

to calculate the recurrence time based on the Gutenberg-Richter's formula, we need to use a large sample to get a reliable conclusion. For instance, the confidence limits of the recurrence time for magnitude ranging from 4.0 to 5.0 will be between 4.3 years to 172 years (under the assumption that the recurrence time for magnitude 4.5 is 1 year and the coefficient b = 1). On the other hand, the estimated confidence limits based on 4000 earthquakes with the magnitude 2 and 3 is between 18.5 years to 52.6 years. If the estimate is made based on even smaller than 50 earthquakes, the range of the confidence limits becomes too great to bear any significant meaning.

(3) It is recognized recently that the level of seismic activity fluctuates significantly under certain circumstances. For instance, a marked decrease of seismic activity is frequently observed prior to a major earthquake. This phenomenon is called the seismicity gap and provides a useful clue to predict a major earthquake (Ohtake et al. 1977). At the time of water filling to a dam, introduction of the water-induced earthquake is frequently experienced. Therefore to apply the results from the Gutenberg-Richter's formula, it is necessary to examine if the sample represents a "stable" period of activity.

5.2 RELATION BETWEEN THE MAGNITUDE SCALES

5.2.1. Ms Versus m_b

Currently two different magnitude scales, m_b (body wave magnitude) and Ms (surface ware magnitude), are widely used. The former, the body wave magnitude, is determined from the maximum amplitude of body waves.

The NEIS earthquake data file reports m_b for almost all the events included in the file. The latter, the surface wave magnitude, on the other hand, is widely used in the engineering application but the NEIS reports Ms only for 15 $\sim$ 20 percent of the events.

As early as in 1956, Gutenberg and Richter found the relation between m_b and Ms as follows:

$$m_b = 2.80 + 0.6\ Ms$$

This relation is still widely used and probably one of the most reliable ones. To find out if this relation holds in Guatemala, the earthquakes that occurred along Central America (63^oW - 80^oW) during the period of 1963 through 1980 were plotted (Figure 7A). The least square fitting provided the following formula:

$$m_b = 2.85 + 0.453\ Ms$$
$$Ms = 2.21\ m_b - 6.29$$

5.2.2. m_b Versus $M\tau$

Another magnitude scale, $M\tau$, which is widely used by many operating networks, is determined from the duration time of the events. For a large event, the maximum amplitude is readily clipped and it is impossible to determine neither m_b nor Ms. $M\tau$, the duration time magnitude, on the other hand, is always applicable. The drawback is that this method requires an empirical formula that connects $M\tau$ to other magnitude scale.

Empirically it is known that the duration time of an earthquake, τ, is correlated to the magnitude of the event in the following form:

$$M\tau = a + b \log \tau.$$

To find out the value of a and b, the duration times of the events with known body wave magnitude, m_b, reported by the NEIS are plotted in Figure 7B. Based on this data, the following empirical formula is given for the duration time magnitude, $M\tau$:

$$M\tau = -2.67 + 3.06 \log \tau \text{ (in sec)}$$

5.3. FREQUENCY - MAGNITUDE RELATION

5.3.1. The NEIS Data File

To examine the level of seismic activity, two sets of data were studied. All the events reported in the NEIS earthquake file during the period from 1963 through 1980 and within the region 89° - 92° West and 12° - 16° North, were counted for in the individual magnitude ranges. Figure 7C shows the plot of the cumulative events count N versus magnitude m_b. The data point shows relatively good linear alignment between m_b = 4.9 and 6.4, but started to fall down below the magnitude m_b = 4.5. This is due to the effect that the regional perceptibility of the WWSSN is approximately 4.5 and some of the events below this magnitude started to escape from being detected. This relation is given as follows:

$$\log N = 7.19 - 1.15\, m_b \text{ (for } 89^{\circ} - 92^{\circ}\text{, 18 years)}$$

If the event count is normalized for the annual count

$$\log N' = 5.93 - 1.15\, m_b \text{ (for } 89^{\circ} - 92^{\circ}\text{, per year)}$$

Based on this relation, the annual count of the events and the recurrence time, 1/N', is calculated and shown in Table 3A.

5.3.2. The Data From Pueblo Viejo-Quixal Network

Figure 7D shows the data located by the Pueblo Viejo-Quixal Network. Two sets of data are shown in this figure. Closed circles show all the events located by the network during the period of February 1979 to March 1981 and closed squares illustrate the events count that were located within 200 km square from the dam site. Closed circles define a lenear trend for the magnitude ranging between 4.6 to 6.0. The count starts to fall down for the events with magnitude smaller than 4.5.

The frequency-magnitude relation is given by:

$$\log N = 6.80 - 1.15\ M_T \quad \textit{(for all events, 2 years)}$$

The closed squares indicate the points within 100 km grid from the dam site and represent the seismic risk in the vicinity of the project area in more direct manner. However, the closed squares show more scattered distribution and it is rather difficult to determine an asymptote. Therefore, the following approach was used: the b-value (slope of asymptote) is assumed to be identical to that determined from closed circles, and draw a line through the data points before it starts to fall down.

With this method, the following relation is acquired:

$$\log N = 6.80 - 1.15\ m_b \quad \textit{(for 200 km grid, 2 years)}.$$

Normalizing to the annual count, we get:

$$\log N' = 6.50 - 1.15\ m_b \quad \textit{(for 200 km grid, per year)}.$$

5.4 RECURRENCE TIME

By the use of the frequency-magnitude relations defined in the

sections (5.3.1.) and (5.3.2.), the recurrence time for the magnitude range between 5.0 to 7.5. The inverse of the normalized annual count, N', gives the recurrence time.

Table 3A gives the recurrence time based on the NEIS data (for the region 89^{o} - 92^{o} West and 12^{o} -16^{o} North) and 3B indicates the recurrence time based on the data from the Pueblo Viejo-Quixal Network (for the grid of 200 km for each side). Throughout the entire magnitude ranges, the letter gives approximately 4 times higher seismicity than the former.

6. ACCLERATION AND INTENSITY

6.1 STRONG MOTION ACCLEROGRAPH OPERATED AT THE DAM SITE

Two sets of 3-component KINEMETRICS SMA-1 strong motion accelographs have been operated at dam site since March 1978. Records for the period between March 1978 and February 1981 are analysed.

Some part of the data was lost because of malfunction of the acclerographs and inadequate loading procedure of the recording film during which the leading and tailing section of the film were subjected to expoure. In addition to loss of the data, the loded time mark is not available for the SMA-1 strong motion acclerograph. These effects made it very difficult for us to identify the recorded events to those recorded by the Pueblo Viejo-Quixal seismic system.

Tables 4A and 4B show the major earthquakes and explosions recorded by SMA-1's during March 1978 through February 1981. Each table shows the recording period on each roll of film, the ID number within the roll, the maximum accleration (measured in g) for longitudinal, vertical and transversal components, and the duration of recognizable amplitudes.

The maximum acclerations recorded by these instruments during the 36 month period are 0.22 g (transversal componant, No. 1, 10 March - 27 April 1978, Table 4B) for site 1 and 0.389g (longitudinal componant, No. 1, 12 August - 28 August 1980, Table 4B) for site 2. However, these two events seem to be generated from explosions.

The maximum accelerations generated by earthquakes are 0.125g (longitudinal componant, No. 3, 1 August - 12 August 1980, Table 4) for site 1 and 0.133g (longitudinal componant, No. 1, 10 March - 27 April 1980, (Table 4A) for site. The duration times of the

recognizable amplitudes of these events are 1.2 and 7.5 seconds respectively.

6.2 CALCULATED ACCELERATION FROM THE NEIS EARTHQUAKE FILE

To compare the accelerations that were recorded at the Pueblo Viejo Dam Site and those calculated from the earthquake file, all the earthquakes that gave the calculated maximum acceleration greater than 0.01g are selected from the NEIS data file and listed in Table 5. The following equation (Esteva, 1973) was used to calculate the peak ground acceleration from given magnitude:

$$a = 5000\ exp(0.8M)\ /\ (HD + 40)^2$$

where a = peak ground acceleration in cm/sec^2
M = magnitude. When both m_b and Ms are given, larger value is used.
HD = hypocentral distance in km

Although this formula was established for the region of California, it was assumed that this formula still provides the first approximation in Guatemala.

Correlations of the events listed in Table 4A and 5 are not quite successful because no absolute time is available for strong motion accelerograms. Only one event (No. 1 of 10 March - 27 April 1978) could be correlated with an earthquake from the NEIS data (30 March 1978, 19h30M, m_b=5.1, hypocentral distance = 47 km). This earthquake gives the largest calculated acceleration at the dam site for the recording period. The calculated acceleration at the dam site from the earthquake of March 30, 1978 is about $40cm/sec^2$ (=0.04g) based on the above formula. The maximum accelerations of this event on the accelerograms are 0.133, 0.033, and 0.065 for longitudinal, vertical, and transverse

component respectively. In most earthquakes, the vertical ground acceleration is ranging from one-third to two-third of the horizontal acceleration. If we assume that the calculated acceleration given by Esteva's formula is for vertical ground acceleration, the calculated and observed maximum accelerations of this event are relatively well correlated each other.

In Table 5, it is interesting to note that the calculated acceleration at the dam site from the 4 February 1976 Guatemala earthquake (m_b= 6.2, Ms = 7.5, HD = 150 km) was 0.057g. One of the largest aftershocks (4 February 1976, 09h 30m, m_b = 5.4, HD = 38.7 km) provided even greater acceleration of 0.062g. This is due to the distance from the dam site, despite the latter was the event with much smaller magnitude.

One of the important conclusions we can draw from Table 5 is that none of the events has exceeded 0.07g during the past 18 years (1963-1980).

6.3. INTENSITY ASSOCIATED WITH THE GUATEMALA EARTHQUAKE OF 4 February 1976

The greatest earthquake that occurred in Guatemala in recent years is 4 February 1976 Guatemala earthquake. The reported surface wave magnitude was 7.5. The intensity distribution associated with this earthquake is shown in Figure 8 (after Espinosa et al., 1976). Intensity VI in the modified Mercalli scale was assigned at the Pueblo Viejo dam site.

There are several churches in the neighboring communities that suffered moderate structural damages but managed to survive from 4 February 1976 earthquake. Figure 9 shows the damages of the church located in San Cristobal Verapaz. It is said that these churches were built cerca 16th century and maintain their original structures. The church in San Cristal Verapaz for instance, reported to have been damaged in 1907 by

an earthquake (not reported in NEIS earthquake file). The reported damages included that some cracks developed on the walls and the room fell down. The structure is primarily made of adobe with very few structural reinforcement. The fact that this church has experienced moderate damages within intensity VI zone support that this structure is classified as Masonry D (poor structure) after C.F. Richter (1958). Such a structure (Masonry D) definitely does not survive for the grand motion of intensity VIII+ to IX. This observation supports the conclusion that the area adjacent to San Cristobal Verapaz never experienced the grand motion equal to or greater than intensity IX in the modified Mercalli scale at least for the past 300 $\sim$ 400 years.

7. CONCLUSION AND RECOMMENDATIONS

7.1. CONCLUSION

The operation of the Pueblo Viejo-Quixal Network and associated studies revealed the following:

A. Two major fault systems, the Motagua fault and Cuilco-Chixoy-Polochic fault, are proved to be active and comprising a complex plate boundary between the North American and the Caribbean plates.

B. Two local linearments, trending N-S and NE-SW respectively, were uncovered in the vicinity of the Pueblo Viejo dam site. The composite fault plane solutions of the events indicate normal faulting and support the interpretation that they are a part of numerous north-south trending sprintering in this region. Based on the recognizable linear extension of 10 km each, the maximum magnitude (Ms) of a possible earthquake expected along these faults are estimated at 5.6.

C. The recurrence time of the regional earthquakes is estimated from both the NEIS earthquake data file and the data from Pueblo Viejo-Quixal Network. The recurrence time for magnitude (m_b) 7.5 are estimated at 501 years and 132 years respectively.

D. The strong motion accelerographs operated at the dam site for the past 2 1/2 years registered the maximum acceleration of 0.133g for the horizontal component and 0.050g for the vertical. The peak (vertical) accelerations for all the major earthquakes since 1963 are calculated based on the NEIS data file. The

calculated peak acceleration associated with the 1976 Guatemala earthquake and one of the largest aftershocks at the dam site are 0.057g and 0.062g respectively. During the past 18 years, no earthquake exceeded the peak acceleration of 0.07g.

E. An old church located in San Cristobal Verapaz suffered a moderate structural damage from the 1976 Guatemala earthquake. The intensity at San Cristobal was VI in the modified Mercalli scale. Based on this observation, it was estimated that this church will not survive the ground motion with the intensity VIII+ to IX. The history of the church (said to have constructed in 16th century) indicates that for nearly the past 400 years, this area has not experienced the intensity greater than IX.

F. It is concluded from the results of the seismic studies (items A through E) that the design criteria for the Pueblo Viejo-Quixal hydroelectric project is adequate for the estimated seismic risk of its life span.

7.2 RECOMMENDATIONS

A. A continued monitoring of the active trends, especially those located in the immediate vicinity of the dam site is of essential importance. In addition, the seismic monitoring program will face another critical phase when impounding of the reservoir starts in late 1981. Before this critical period starts, it is necessary to remedy all the problems and bring the network in the top condition.

B. For this purpose, we need to improve the following procedures:

B.1. Examination of the station performance and rapid

identification of the problem both by INDE and UT personnels.

B.2. Prompt response of INDE's maintenance crew to remedy a malfunction when the problem is identified.

B.3. Improvement of the technical background for INDE's maintenance crew, including sending a technician to Galveston for short-term training.

B.4. More frequent visits by UT technicians for maintenance.

LIST OF TABLES

TABLE 1. LIST OF STATIONS OF PUEBLO VIEJO-QUIXAL SEISMOGRAPH NETWORK

NO.	LONG (DEGREE)	LAT (DEGREE)	ELEVATION (KM)	NAME	REMARK
1	90.49W	15.35N	1.702	Chilley	13 Feb. 1979 - Present
2	90.47W	15.29N	1.180	San Juan	13 Feb. 1979 - Present
3*	90.44W	15.32N	1.560	Panrum	13 Feb. 1979 - 28 Apr. 1979
	90.54W	15.31N	1.860	Cerro San Juan	29 Apr. 1979 - Present
4	90.28W	15.39N	1.650	Xucaneb	13 Feb. 1979 - Present
5	90.50W	15.46N	1.960	Najitila	13 Feb. 1979 - Present
6	90.69W	15.26N	2.220	Chimagua	13 Feb. 1979 - Present
7†	90.50W	15.19N	1.020	Chitucan	13 Feb. 1979 - 28 Apr. 1979
	90.41W	15.00N	2.290	Chiquihuital	29 Apr. 1979 - 4 Oct. 1979
	90.43W	15.09N	1.480	Cerro Champerez	5 Oct. 1979 - Present

* Station 3 relocated on 28 April 1979

† Station 7 relocated on 28 April 1979 and on 5 Oct. 1979

TABLE 2. THE NUMBER OF EVENTS CLASSIFIED BY IQ

(From 13 February 1979 through 10 March 1981)

IQ	1	2	3	4	5	6	7
N	74	344	461	903	2096	263	212

TOTAL NUMBER RECORDED 4357

TABLE 3A. RECURRENCE TIME

Based on the NEIS data file, for 89^{o} - 92^{o} West and 12^{o} - 16^{o} North

$\log N' = 5.93 - 1.15\, m_b$, $R(\text{Recurrence Time}) = 1/N'$

m_b	5.0	5.5	6.0	6.5	7.0	7.5
$\log N$	0.18	-0.40	-0.97	-1.55	-2.12	-2.70
N'(per Year)	1.51	0.40	0.11	0.029	0.0076	0.0002
R(year)	.66	2.5	9.3	35	132	501

TABLE 3B. RECURRENCE TIME

Based on the Pueblo Viejo-Quixal Network data, within 200km square from the dam site

$\log N' = 6.50 - 1.15\, M\tau$, $R(\text{Recurrence Time}) = 1/N'$

$M\tau$	5.0	5.5	6.0	6.5	7.0	7.5
$\log N$	0.75	0.18	-0.40	-0.97	-1.55	-2.12
N (per year)	5.62	1.51	0.40	0.11	0.029	0.0076
R (year)	.18	.66	2.5	9.3	35	132

TABLE 4A. OBSERVED MAXIMUM ACCELERATIONS FROM EARTHQUAKES (g)

DATE	SITE 1 (LEFT)					SITE 2 (RIGHT)				
	NO.	L	V	T	D	NO.	L	V	T	D
3/10 - 4/27,1978	1	-	0.042	0.042	2.5	1	0.133	0.033	0.061	7.5
8/18 - 8/19,1978						1	0.042	0.028	0.033	4.8
9/10 -10/30,1978						1	0.031	0.008	0.014	0.6
						2	0.028	0.006	0.014	3.5
						3	0.036	0.011	0.019	1.3
						4	0.050	0.014	0.028	4.5
						5	0.028	0.006	0.008	3.8
						6	0.031	0.006	0.014	5.0
3/14 - 7/12,1979	1	0.025	-	0.028	1.4					
	2	0.111	-	0.089	1.5					
	3	0.069	-	0.061	1.5					
	4	0.050	-	0.017	0.8					
	5	0.022	-	0.019	1.1					
	6	0.019	-	0.014	1.2					
6/20 - 8/30,1979	1	0.022	0.028	0.028	0.7	1	0.028	0.014	0.003	1.1
	2	0.014	0.006	0.014	0.7	2	0.028	0.014	0.006	4.5
	3	0.025	0.006	0.028	0.8	3	0.028	0.006	0.022	2.4
	4	0.017	0.003	0.014	1.0	4	0.028	0.022	0.006	0.7
	5	0.017	0.006	0.022	1.0	5	0.056	0.042	0.028	0.6
	6	0.028	0.014	0.028	1.0	6	0.014	0.008	0.003	2.2
	7	0.028	0.008	0.022	1.1					
	8	0.022	0.003	0.022	1.0					
	9	0.028	0.003	0.017	0.9					
	10	0.056	0.006	0.022	1.0					
1/27 - 5/28,1980 (A)	1	0.003	-	0.008	1.0					
6/26 - 8/21,1980 (A)	1	0.014	-	0.008	1.5					
8/1 - 8/12,1980 (A)	1	0.019	0.014	0.014						
	2	0.053	0.017	0.033	1.9					
	3	0.125	0.042	0.052	1.2					
	4	0.069	0.042	0.069	2.5					
	5	0.056	0.028	0.050	0.7					
	6	0.056	0.028	0.022	1.6					
	7	0.033	0.017	0.019	2.0					
	8	0.028	0.019	0.014	1.2					
8/12 - 8/28,1980	1	0.033	0.042	0.061	0.6					
	2	0.011	0.016	0.028	0.7					

Cont'd Table 4A

DATE	SITE 1 (LEFT)					SITE 2 (RIGHT)				
	NO.	L	V	T	D	NO.	L	V	T	D
10/10 - 10/24,1980	1	0.019	0.022	0.033	0.7					
	2	0.002	0.008	0.028	0.8					
10/24 - 11/14,1980	1	0.028	0.014	0.033	1.1					
11/14 - 12/30,1980	1	0.025	0.022	0.039	1.1	1	0.014	0.003	0.006	2.2
	2	0.028	0.028	0.028	1.1					
	3	0.056	0.042	0.086	1.6					
12/3 - 1/18,1980	1	0.056	0.042	0.064	1.5					
	2	0.026	0.008	0.014	0.8					
	3	0.022	0.006	0.022	0.8					
	4	0.019	0.014	0.031	1.2					
1/18 - 2/11,1981	1	0.056	0.033	0.083	1.5	1	0.014	0.014	0.014	0.9
	2	0.055	0.050	0.078	1.6	2	0.008	0.006	0.014	1.2
2/11 - 2/27,1981	1	0.053	0.022	0.028	1.5					

* Abbreviations:

L = Longitudinal component (g)
V = Vertical component (g)
T = Transverse component (g)
D = Total signal duration (sec)

(A) ID number is not known

TABLE 4B. OBSERVED MAXIMUM ACCELERATIONS FROM EXPLOSIONS (g)

DATE	SITE 1 (LEFT)					SITE 2 (RIGHT)				
	NO.	L	V	T	D	NO.	L	V	T	D
3/10/ - 4/27,1978	1	-	0.086	0.222	1.3	1	0.167	0.039	0.078	1.2
	2	-	0.139	0.097	0.3	2	0.161	0.075	0.081	0.9
	3	-	0.167	0.083	0.3	3	0.267	0.194	0.139	0.4
11/78 - 3/14,1979	1	0.031	0.092	0.119	1.8					
	2	0.050	0.086	0.128	1.8					
8/12 - 8/28,1980	1	0.058	0.067	0.153	1.0	1	0.389	-	0.111	1.4
						2	0.111	-	0.031	1.0
						3	0.139	-	0.028	1.2
						4	0.111	-	0.028	1.2
8/28 - 9/10,1980							0.119	-	0.032	1.4
10/10 - 10/24,1980	1	0.139	0.222	0.250	1.5					
	2	0.058	0.061	0.222	1.8					

* Abbreviations (see Table 4A)

FIGURE CAPTIONS

Figure 1. Description of the Pueblo Viejo-Quixal Seismograph Network

Figure 2. System diagram

Figure 3A. Down time chart of the network

Figure 3B. Down time chart of the network

Figure 3C. Down time chart of the network

Figure 4. Regional distribution of Earthquakes

Figure 5A. Distribution of earthquakes in the vicinity of the projected area.

Figure 5B. Distribution of earthquakes in the vicinity of the projected area.

Figure 6. Composite fault plane solutions

Figure 7A. Ms versus m_b

Figure 7B. M_τ versus m_b

Figure 7C. Frequency-magnitude relation from the NEIS data

Figure 7D. Frequency-magnitude relation based on the data from the Pueblo Viejo-Quixal Seismograph Network

Figure 8. Intensity Distribution of 4 February 1976 Guatemala Earthquake (after Espinosa et al. 1976)

Figure 9. Damages caused by the Guatemala earthquake of 4 February 1976 at San Cristobal Verapaz

PUEBLO VIEJO-QUIXAL SEISMOGRAPH NETWORK

FIG. 2

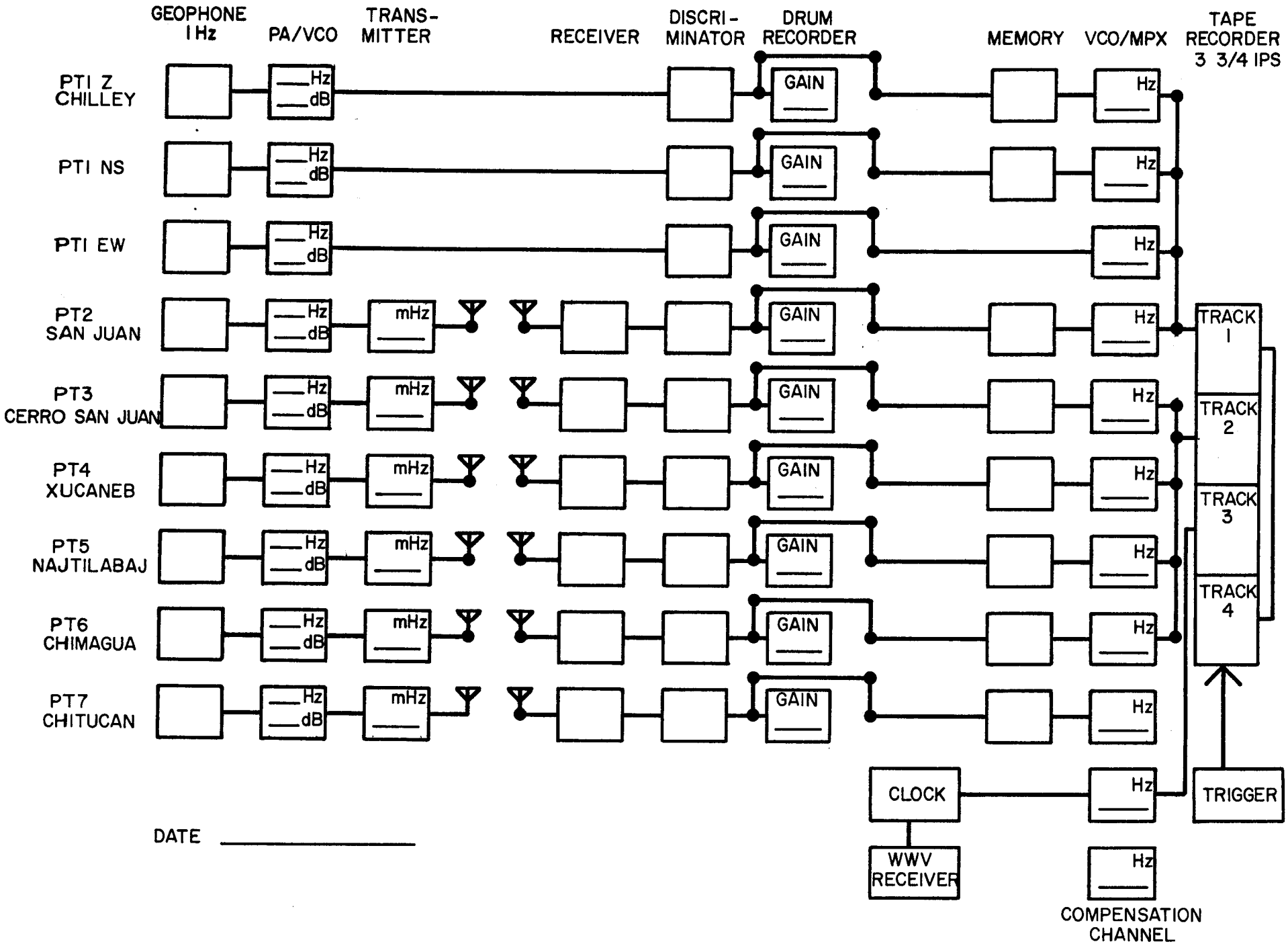

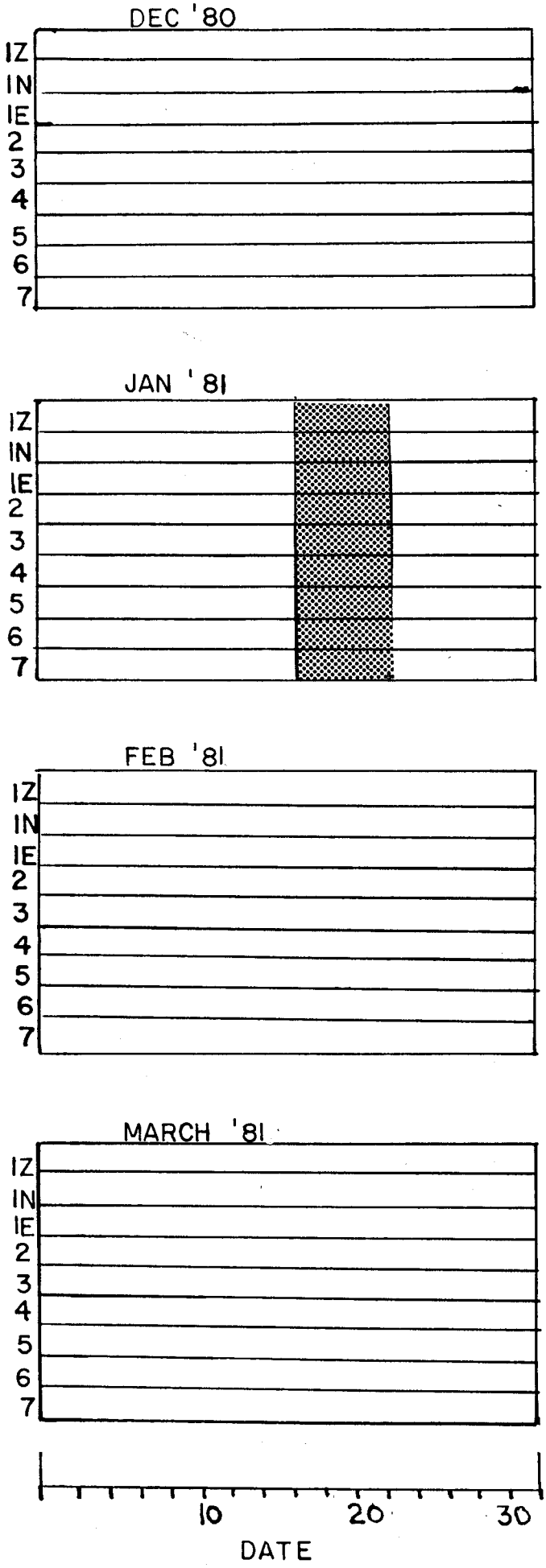

NOTES

Fig. 3A

(1) Station 4 drum record recording good events all month.
(2) Pen traces good.

(1) 5 stations recording good on tape
(2) Excellent time code on tape
(3) Short period time mark installed Jan. 20

(1) Long period time mark installed Feb. 10.

(1) Data received up to March 10 only.

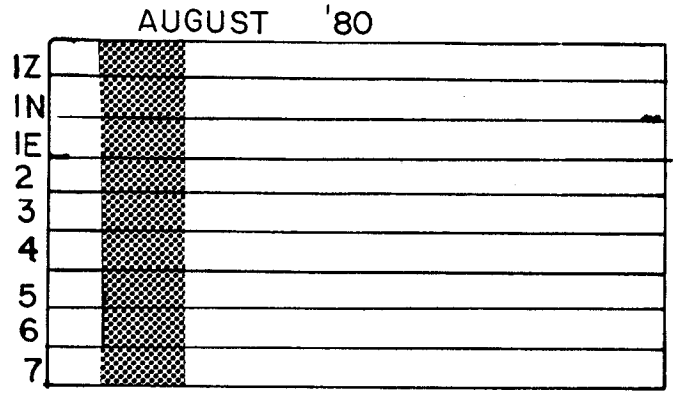

NOTES

Fig. 3B

(1) Station 4 drum record started as of 8-1-80, but no events recorded.
(2) Station 1EW drum record started Aug. 5 with good recording.
(3) Station 6 drum record started Aug. 5, but no events recorded.

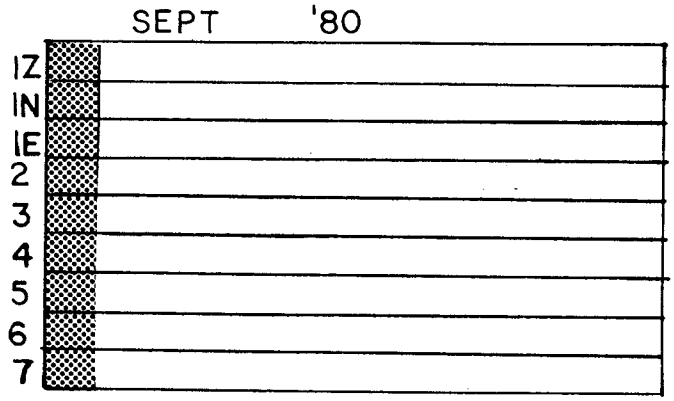

(1) Station 6 began recording good events on the drum Sept. 18
(2) Pen trace very nice on all stations.

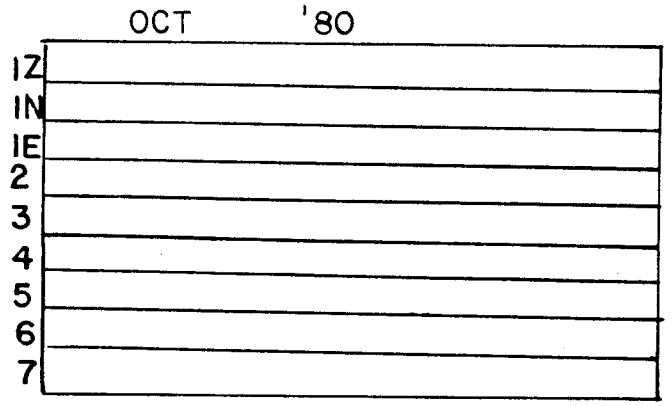

(1) 5 stations operating well on tape recording system
(2) Station 6 drum record recording good events whole month.
(3) No drum record station 2, 7.
(4) All pen traces very nice.

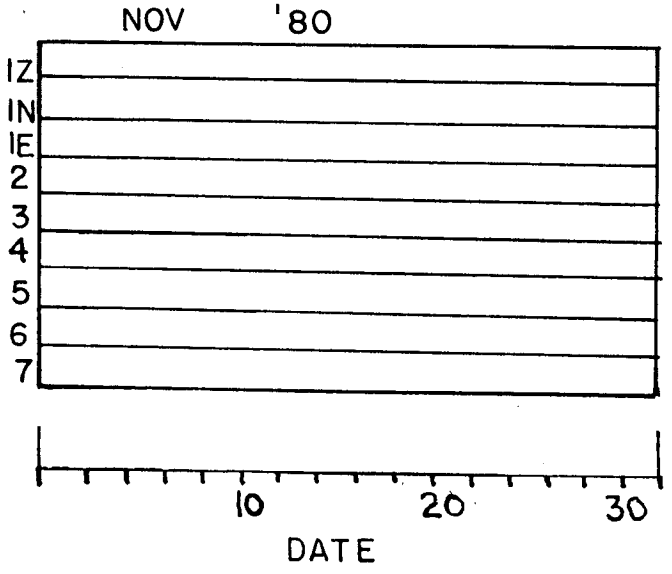

(1) Station 6 drum record shows events clipped on +125 Hz side.
(2) Station 12, 1N, 1E drum records very good.
(3) No drum records station 2 or 7
(4) Pen traces good
(5) Time code resumed on tape as of Nov. 1.

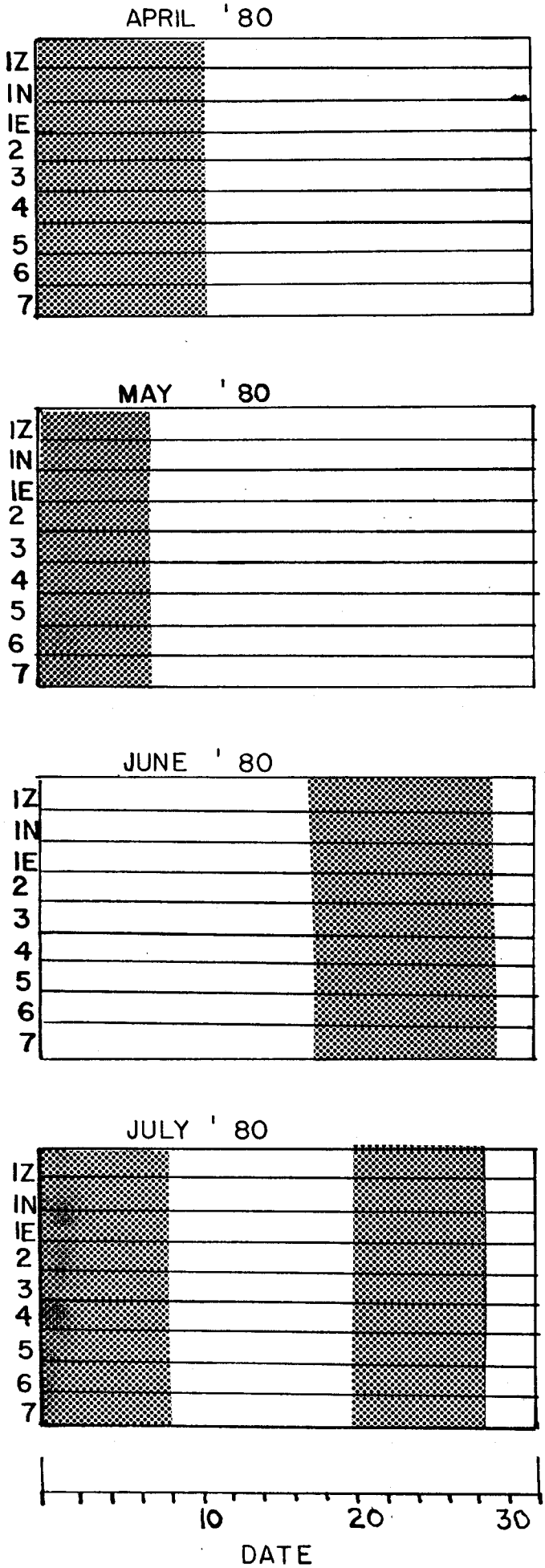

NOTES

Fig. 3C

(1) No time code on the tape at all
(2) No time code on Drum Records from 4-1 to 4-10
(3) No Drum Record IN, 4, 6, 7

(1) No time code on the tape at all
(2) No drum record for point IN, 4,7

(1) No time code on the tape at all
(2) No drum record IN, IE, 4,7

(1) No time code on the tape at all

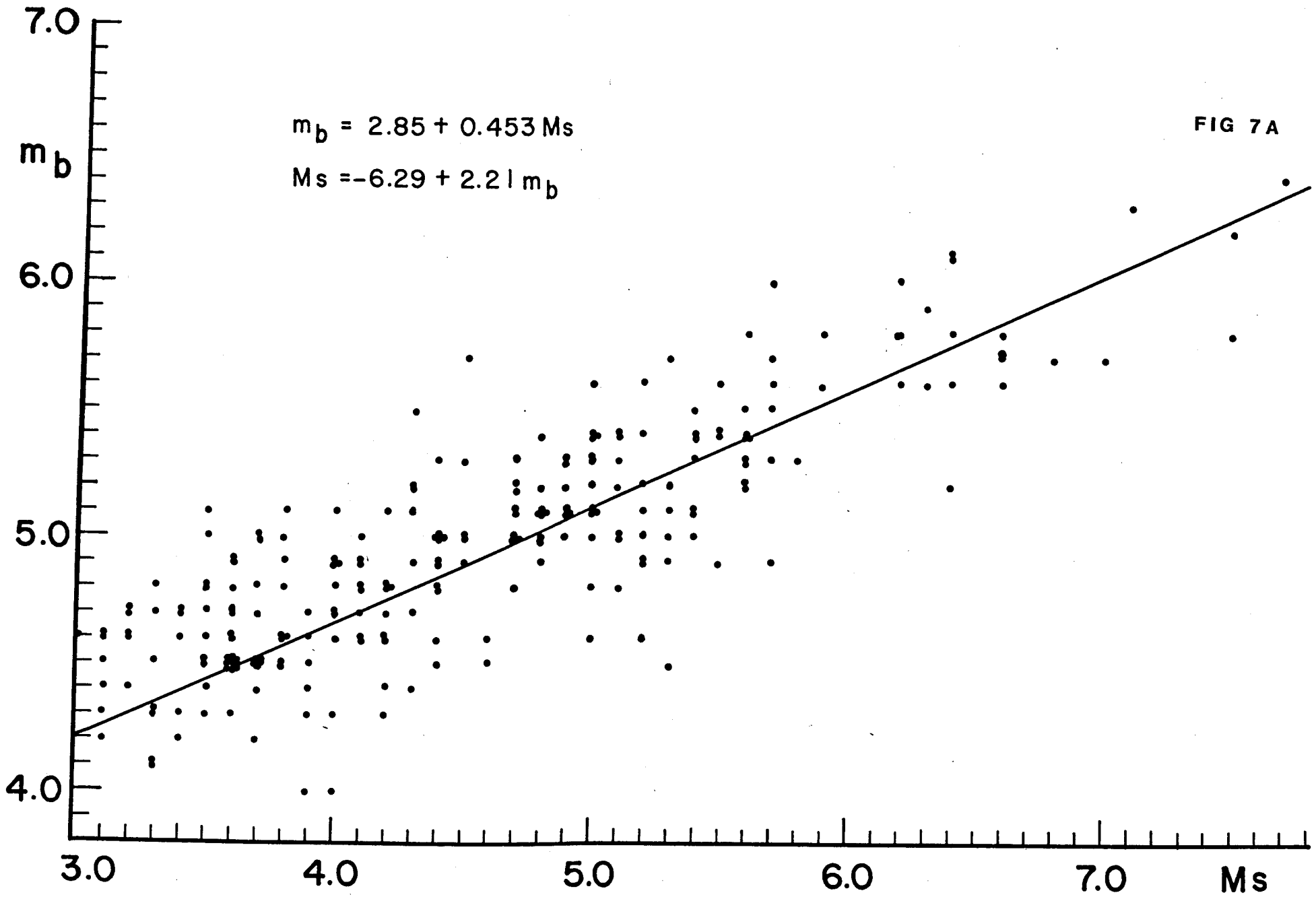

FIG 7A

PUEBLO VIEJO-QUIXAL NETWORK

FIG. 7D

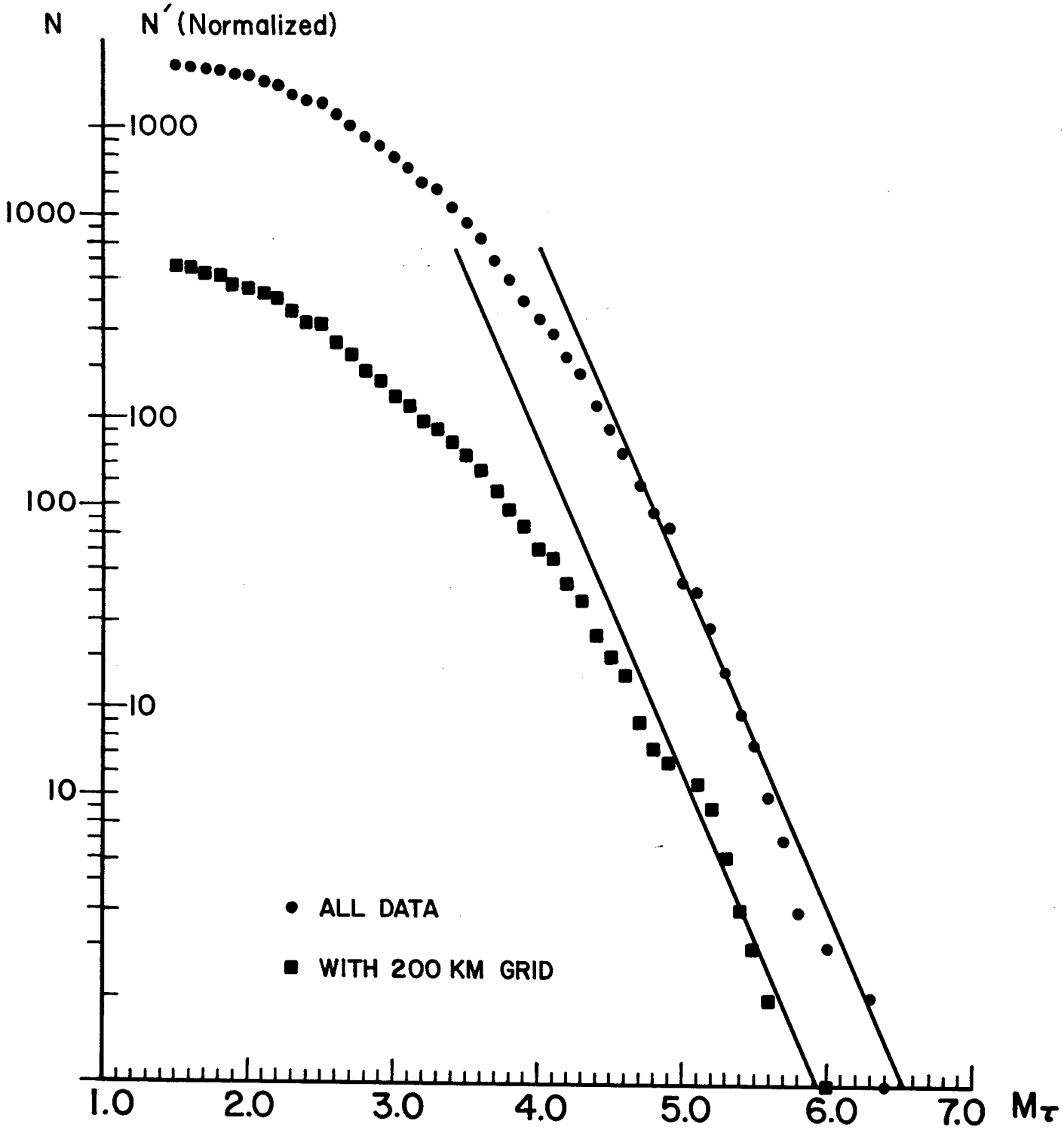

Appendix. List of earthquakes recorded by the Pueblo-Chixoy-Quixal-Seismograph Network.

Column	Abbreviation	Description
1	NO	Identification number
2	YR	Year
3	M D	Month and Day
4	H M	Hour and minutes, G.M.T. (to calculate local time, subtract 6 hours)
5	S	Second of the origin time, a decimal point should be assumed between 2nd and 3rd digit
6	NP	Number of P-arrival reading
7	NS	Number of S-arrival reading
8	IQ	Quality number, ranging 1 through 5, 1 being the most accurate reading
9	ITR	Number of iterations carried out during the epicenter calculations
10	MAG	Magnitude x10, magnitude is calculated based on the duration time.
11	LONG	Longitude of epicenter (in degree)
12	LAT	Latitude of epicenter (in degree)
13	X	Distance measured from the central station (eastward positive)
14	Y	Distance measured from the central station (northward positive)
15	DEPTH	Depth; if a negative depth is obtained during the iteration process, the epicenter program automatically fixes the depth at 5.0 km and x, y are calculated.
16	DX	Standard error for X (in km)
17	DY	Standard error for Y (in km)
18	DZ	Standard error for Z (in km)
19	S	Standard error for origin time (in sec)